Optics Communications 359 (2016) 129–134

Contents lists available at ScienceDirect

Optics Communications

journal homepage: www.elsevier.com/locate/optcom

Coupling structure for silicon slot waveguide operating at 1064 nm

Xiangdong Li, Xue Feng*, Xian Xiao, Yihang Li, Kaiyu Cui, Fang Liu, Yidong Huang

Department of Electronic Engineering, Tsinghua National Laboratory for Information Science and Technology, Tsinghua University, Beijing 100084, China

ARTICLE INFO

Article history:
Received 19 March 2015
Received in revised form
26 August 2015
Accepted 13 September 2015

Keywords:
Silicon photonic integrated circuits
Silicon slot waveguide
Coupling
High absorption
Refraction

ABSTRACT

A coupling structure with a shape of isosceles trapezoid is experimentally demonstrated for injecting lightwave into silicon slot waveguide operating at 1064 nm. A transfer waveguide is adopted to mimic a silicon emitter and the coupling losses of varied mode sizes of incident lightwave are measured. According to experimental results, the low coupling loss region of "<1 dB" is obtained with varied structural parameters. Furthermore, the loss mechanism of our proposed coupling structure is also analyzed.

1. Introduction

Silicon photonics have always been attracting much interest and made a great progress in the last decade since it is possible to merge both electronics and photonics on a single silicon chip [1,2]. Most of the reported silicon photonic devices operate at the optical communication wavelength around 1550 nm [3]. Actually, it should be noticed that the silicon devices operating at shorter wavelength have entered in the scope of researchers [4,5]. Based on the achievement of silicon emitters [6,7], it is possible to obtain all-silicon photonic integrated circuit (PIC) system with mature complementary metal-oxide-semiconductor (CMOS) fabrication process [8]. Meanwhile, the operating wavelength of material processing and biological applications are primarily at 1064 nm [9,10] and the operation window for optical trapping of biological cells and small organisms is 750–1200 nm [11]. It would be very attractive to apply silicon photonic devices and technology on the aforementioned applications to take the advantages of multi-functionality, low power consumption, and massive production. For all-silicon PIC, the operating wavelength should be less than 1.1 μm, which is determined by the silicon emitter. It is well known that light would be highly absorbed by silicon material within such wavelength band [12]. Thus, the main challenge to achieve all-silicon PIC is how to deal with the material absorption loss. One feasible solution is utilizing slot waveguide as proposed in our previous work [13]. A slot waveguide consists of two strips with high refractive index and one slot with low refractive index, in which the light is confined within slot region and thus the absorption of strip material is not so crucial for the transmission loss of the waveguide. Moreover, slot waveguide could also be adopted for signal processing [14], optical manipulation [15] and chemical/biological sensing [16,17] due to the high confinement of lightwave [18]. In order to serve as the infrastructure of PIC, it is required to couple lightwave from silicon emitter into a slot waveguide efficiently. Such coupling would be more complicated than a traditional coupling structure since the mode mismatch as well as high material absorption should be considered [19,20].

In this paper, we have experimentally investigated the coupling structure that could efficiently inject lightwave into a slot waveguide at operating wavelength of 1064 nm. In general, the mode size of emitter is several micrometers, which is quite larger than that of slot waveguide [5]. As a first step, a set of transfer waveguides with width of 2–6 μm is adopted to take the place of a silicon emitter while the width of slot region of slot waveguide is constant as 100 nm. Considering the mode mismatch and high material absorption, the coupling structure is designed as isosceles trapezoid shape. With varied parameters of the coupling structure, the coupling losses between different transfer waveguides and slot waveguide are measured. The coupling loss could be as low as about 0.3–4 dB. According to experimental results, the "<1 dB" region and the mechanism of coupling loss are discussed and analyzed while some guidelines of designing coupling structure are presented. We believe that this work provides an approach for efficiently coupling lightwave into a silicon slot waveguide at high material absorption band and takes a step towards the all-silicon PIC.

* Corresponding author. Fax: +86 10 62797073-801.
E-mail address: x-feng@tsinghua.edu.cn (X. Feng).

http://dx.doi.org/10.1016/j.optcom.2015.09.048
0030-4018/

2. Structure and fabrication

In our previous work [13], the silicon slot waveguide has been fabricated and measured. Considering the high silicon absorption at the operating wavelength, a SiO_2 transfer waveguide is introduced to take the place of silicon emitter with the wider mode size. Fig. 1(a) shows the schematic of the fabricated sample. There is a slot waveguide with one coupling structure at each end connected to a transfer waveguide. The mode coupled from fiber is converted to the propagation mode of the transfer waveguide with different sizes according to the width of transfer waveguide *w*. The slot waveguide consists of two silicon strips filled with and surrounded by SiO_2, and the widths of two strips and slot region are all 100 nm, which agrees with our previous work [13]. The mode field and the electric field distribution along *x*-axis (Fig. 1(a)) of slot waveguide are shown in Fig. 1(b) and (c), respectively. These results show that the mode size of slot waveguide is nearly as same as the width of slot region but quite smaller than the typical mode size of a silicon emitter (~μm). The lengths of the slot waveguide, coupling structure, and transfer waveguide are denoted as L_s, L_c, and L_t, respectively. As shown in Fig. 1(a), the shape of coupling structure is isosceles trapezoid and the width of the broadside is *w* while the corresponding oblique angle is θ. It should be mentioned that the core materials of both transfer waveguide and coupling structure are designed as SiO_2 to reduce the transmission loss. Since the refractive index of SiO_2 is lower than that of Si, the optical confinement would be weakened. Such impact on the transfer waveguide does not matter because the transfer waveguide is used to mimic a silicon emitter and the transmission loss would be deducted from the result. For coupling structure, the impact of SiO_2/Si interface would be discussed in the last part of this paper.

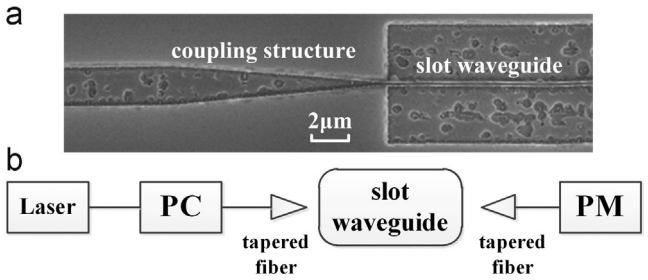

Fig. 2. (a) The SEM image of a fabricated sample with coupling structure and slot waveguide. (b) The schematic setup of measurement system.

The samples are fabricated on a SOI wafer with a 220 nm top silicon layer and a 3 μm buried oxide layer. Thus, the heights of all the silicon waveguides are 220 nm. The pattern is defined with electron beam lithography (EBL). All the waveguides are etched with inductively coupled plasma reactive ion etch (ICP-RIE), and then covered by a SiO_2 cladding layer through plasma enhanced chemical vapor deposition (PECVD). Fig. 2(a) is the scanning electron microscope (SEM) image of one fabricated coupling structure without SiO_2 cladding.

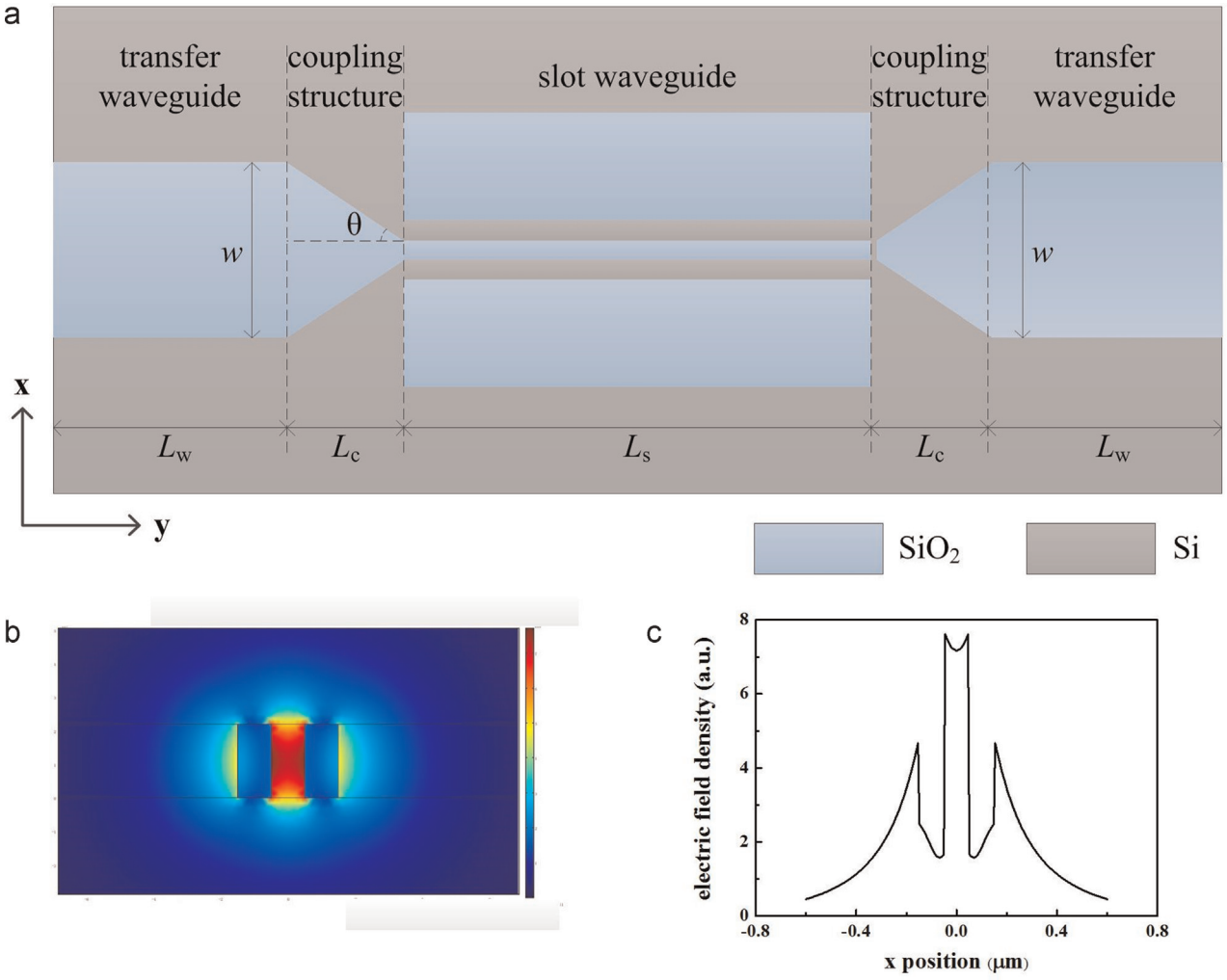

Fig. 1. (a) The schematic of the sample. The mode profile (b) and the electric field distribution (c) of slot waveguide.

Following our previous work [13], the operating wavelength is also 1064 nm, where the material absorption of bulk silicon is as high as ~5 dB/mm [12]. The prepared samples are characterized with a common system as shown in Fig. 2(b), including a 1064 nm laser, a polarization controller (PC), and a power meter (PM). Two single-mode lensed optical fibers, mounted on a computer-controlled alignment stage, are used to couple light in and out of the waveguides. The output power of the laser source is set as a constant value of 1 mW (0 dBm). Here, only the transmission loss of TE polarization is measured, because the transmission loss of slot waveguide for TM is much higher than that for TE [13]. In experiment, the polarization of light coupled out from the lensed fiber is aligned utilizing a single mode waveguide. By subtracting the output power of the system from the laser output, the total transmission loss of the entire system (β_e) is obtained. Obviously, the measured result is the sum of transmission loss of slot waveguide ($\beta_s=\alpha_s L_s$), transfer waveguide ($\beta_t=\alpha_t L_t$), the coupling loss of two identical coupling structures (β_c), and other losses (β_o) which includes the insertion loss of PC and the coupling losses between the lensed fibers and sample. Thus, the measured result could be expressed as:

$$\beta_e = \alpha_s \cdot L_s + \alpha_t \cdot L_t + \beta_c + \beta_o \quad (1)$$

And the coupling loss can be expressed as:

$$\beta_c = \beta_e - \alpha_s \cdot L_s - \alpha_t \cdot L_t - \beta_o \quad (2)$$

In order to obtain the coupling loss of the coupling structure, the values of β_e, α_s, α_t and β_o should be first determined. For this purpose, three groups of samples are fabricated and the details are shown in Table. 1. In Group 1, there are only slot waveguides with varied lengths so that the attenuation coefficient of slot waveguide (α_s) could be obtained by linear fitting the measured data. In Group 2, there are only transfer waveguides with varied both lengths (L_t) and widths (w) in order to calculate the values of α_t and β_o. In Group 3, each sample includes all the structures shown in Fig. 1(a), where the coupling structures with varied widths (w) and oblique angles (θ) are fabricated. Here, the different widths w (2 μm, 4 μm, and 6 μm) in Group 2 and 3 are in order to investigate the coupling between slot waveguide and different-size modes. And different angles θ under each w are designed in Group 3 to reveal the dependence of coupling loss on θ and achieve low loss coupler structure. It should be mentioned that all samples of three groups are fabricated on the same wafer and cleaved at the same time. Thus, we assume that the coupling loss between the lensed fiber and transfer waveguide is only dependent on the waveguide width (w) in despite of samples in Group 2 or Group 3. Then, after the value of β_o is obtained by measuring the samples of Group 2, such value would be applied for the corresponding samples of Group 3 with the same transfer waveguide width.

3. Measurement and results

In order to make sure the light transmits through the corresponding waveguide, the output power under different input position and output position along the x-axis in Fig. 1(a) is measured for each measurement. One typical normalized output spectrum under different input positions is shown in Fig. 3. The position 0 μm in Fig. 3 shows where maximum output is achieved. The output under varied output position with constant input position is similar. These measurements indicate that the light have been coupled into the waveguide.

Table 1
The structural parameters of fabricated samples.

Group	1	2	3
L_s (mm)	2.0/2.5/3.0	0	1
L_t (mm)	0	2.0 / 2.5 / 3.0	2
Coupling structure	No	No	Yes
w (μm)	–	2/4/6	2/4/6
θ (°)	–	–	5/10/15
Number	5 per L_s	5 per L_t per w	3 per w per θ

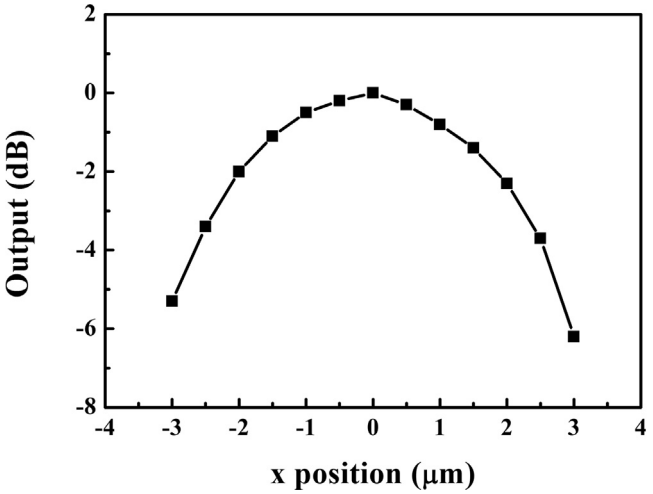

Fig. 3. Normalized output spectrum under varied input position.

First, the attenuation coefficient of silicon slot waveguide (α_s) is measured. As shown in Group 1 of Table 1, three lengths of L_s=2.0 mm, 2.5 mm, and 3.0 mm are adopted and there are five samples for each length. The measured results are shown in Fig. 4, in which each square represents the average value of the five samples and the error bar represents the corresponding standard deviation. By linear fitting, the solid line is obtained as $\beta_e=2.28\times L_s+35.1$. And the slope of fitting line represents the attenuation coefficient as 2.28 ± 0.03 dB/mm. Thus, α_s=2.28 dB/mm is adopted in the following step. In addition, the intercept of the fitting line (~35.1 dB) indicates the total transmission loss of system with L_s=0, including the coupling losses between slot waveguide and two lensed fibers as well as the insertion loss of PC. After subtracting the insertion loss of PC (~2 dB), the single-side coupling loss between slot waveguide and lensed fiber is estimated as high as 16.5 dB.

Secondly, the samples of Group 2 are measured. The widths of transfer waveguide are w=2 μm, 4 μm, and 6 μm and the

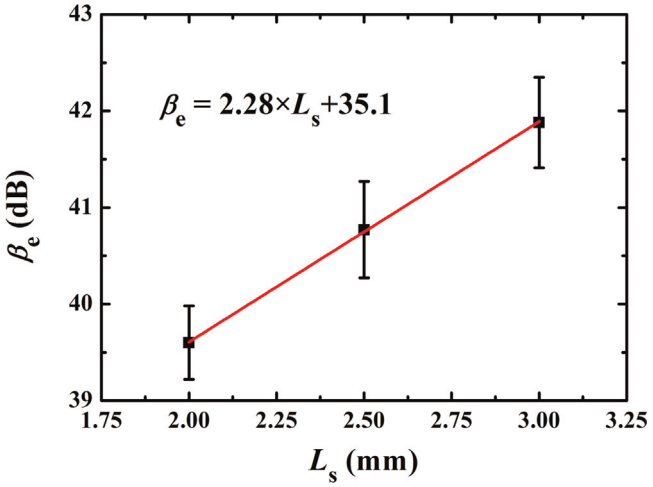

Fig. 4. Measured total transmission losses β_e of slot waveguides.

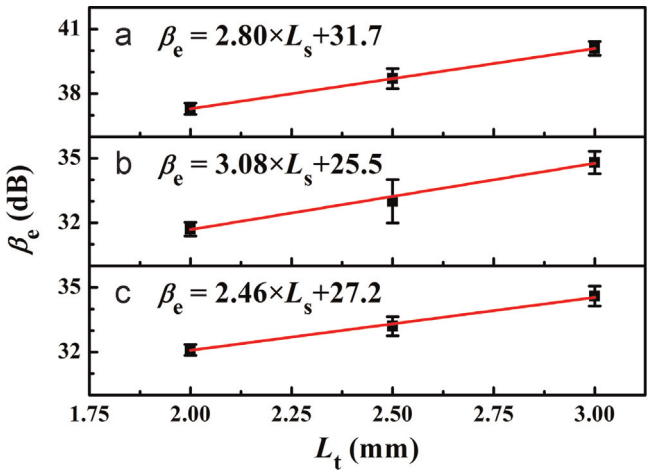

Fig. 5. Measured total transmission losses β_e of transfer waveguides with $w=2$ μm (a), 4 μm (b) and 6 μm (c), respectively.

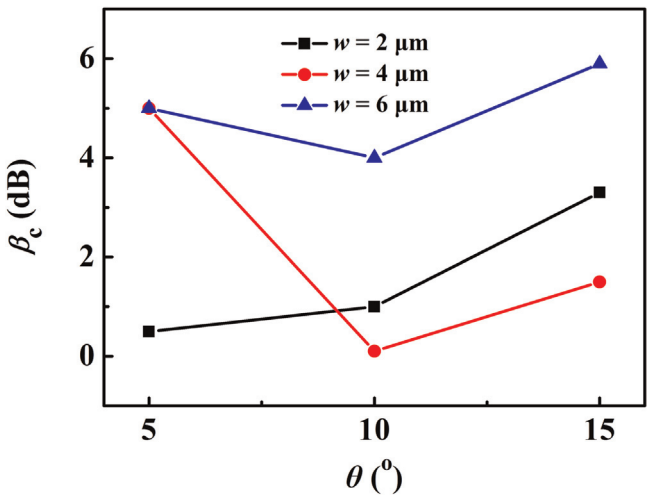

Fig. 6. The coupling losses versus the angle θ under different w.

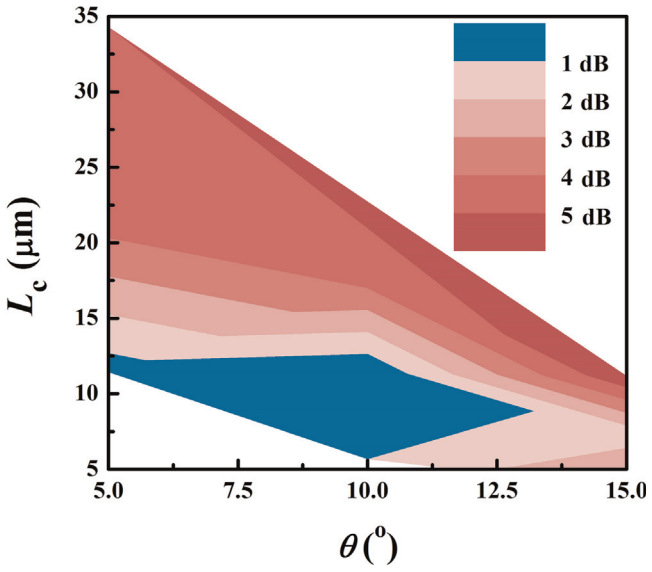

Fig. 7. Gray scale map of coupling losses under different lengths L_c and angles θ. (For interpretation of the references to color in this figure, the reader is referred to the web version of this article.)

measured transmission losses are shown in Fig. 5(a)–(c), respectively. For each length, there are also five identical samples. Similar to Fig. 4, the transmission loss coefficient α_t is also obtained by linear fitting. According to the results shown in Fig. 5, the fitting lines are $\beta_e=2.80\times L_s+31.7$, $\beta_e=3.08\times L_s+25.5$, and $\beta_e=2.46\times L_s+27.2$ for three cases. Thus, $\alpha_t=2.80$ dB/mm, 3.08 dB/mm, and 2.46 dB/mm are adopted for the transfer waveguides of $w=2$ μm, 4 μm, and 6 μm, respectively. In theory, α_t should decrease as w increases. But the experimental results are a little different. The value for $w=4$ μm (3.08 dB/mm) is a little higher than that for 2 μm (2.80 dB/mm). Such abnormal results may come from the fabrication and measurement errors, there is a possible interpretation from the fact that the error bars of experimental results for $w=4$ μm are higher. Similarly, the other losses (β_o) could be achieved from the intercepts of the solid lines in Fig. 5 and the results are $\beta_o=31.7$ dB, 25.5 dB, and 27.2 dB, respectively.

After β_e, α_s, α_t and β_o are determined, the coupling loss of slot coupling structure can be determined. In order to investigate the coupling between slot waveguide and silicon emitters with different-size modes, the widths of transfer waveguides are $w=2$ μm, 4 μm, 6 μm. And for each w, different angles ($\theta=5°$, 10°, and 15 °) are designed. For each type, the values of α_s, α_t and β_o are shown in Table 2. In experiment, for each type of the coupling structure, there are three identical samples and the final result of β_e is the average value of them. The length of slot waveguide L_s is 1 mm, and the two transfer waveguides, including input and output part, are both 1 mm long, which is long enough to insure the light has been transferred into the mode, whose size is in keeping with w. Thus the coupling loss β_c of two coupling structures could be calculated according to Eq. (2). Fig. 6 shows that the coupling loss versus θ under different w. It is obvious that for different-size modes (w), there are different optimized θ according to experimental results. That is, the coupling structure of slot waveguide should be designed according to the objective mode. The losses of the coupling structures with $w=2$ μm, 4 μm, and 6 μm could be as low as 0.5 dB, 0.3 dB and 4 dB, respectively. In order to get deep insight of the coupling mechanism behind the results shown in Fig. 6, some calculations and further analysis have been done.

For more clarity, the coupling loss versus L_c ($L_c\approx w/(2\tan\theta)\approx w/(2\theta)$) and θ is re-plotted as gray scale map in Fig. 7. It could be found that the coupling loss is low within a certain region. As shown in the blue region in Fig. 7, $\beta_c<1$ dB. Thus, the "$<$ 1 dB region" could be considered as about $\theta<12°$ and $L_c<12$ μm, which means that both of the oblique angle and the length of coupling structure should be small. Thus, in order to

Table 2
α_s, α_t and β_o for each type of coupling structure.

α_s (dB/mm)/α_t (dB/mm)/β_o (dB)		w (μm)		
		2	4	6
θ (°)	5	2.28/2.80/31.7	2.28/3.08/25.5	2.28/2.46/27.2
	10	2.28/2.80/31.7	2.28/3.08/25.5	2.28/2.46/27.2
	15	2.28/2.80/31.7	2.28/3.08/25.5	2.28/2.46/27.2

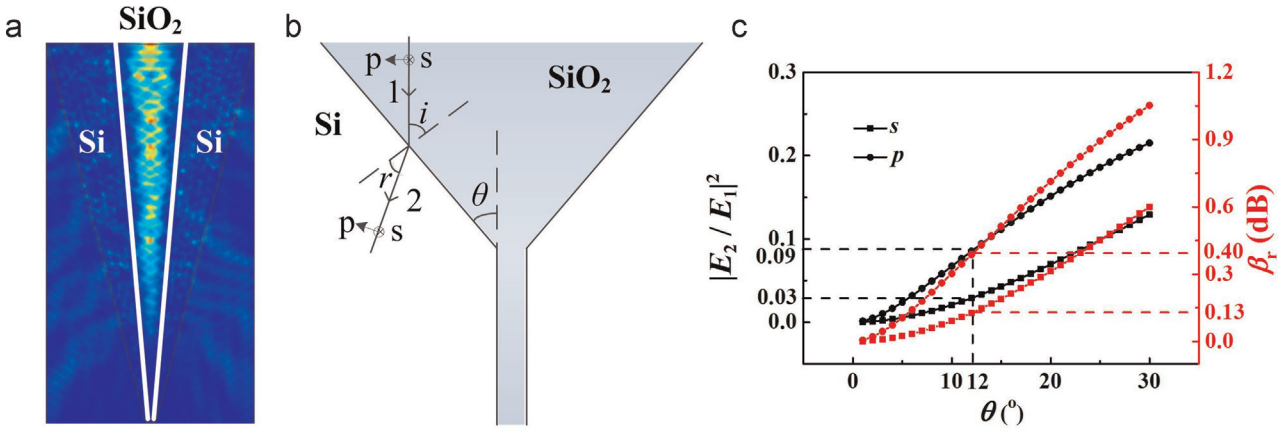

Fig. 8. (a) The transmission mode in the coupling structure. (b) The simplified schematic diagram of the coupling structure. (c) The ratio between refracted light and incident light versus the angle θ.

realize low loss coupling loss (<1 dB), the size of mode satisfies $w \approx 2\theta L_c < 5$ μm approximately. The white region represents lack of experimental results.

In terms of length L_c, it is quite obvious since longer length would introduce more absorption and scattering loss. However, for oblique angle θ, it is not so intuitive to understand the results. For deep insight, some calculations are carried on. First, the transmission mode in the coupling structure is simulated and the result is shown in Fig. 8(a). Here, though only two-dimensional calculation is carried out, some qualitative characteristics of the propagation mode could also be obtained. Fig. 8(a) shows that a small fraction of light would enter silicon region from SiO_2 while propagating within the coupling structure. Thus, in our coupling structure, since the light transmits from SiO_2 (low refractive index) into silicon (high refractive index), the additional loss introduced by refraction (β_r) should be considered. The coupling structure is simplified as shown in Fig. 8(b). The light ray 1 represents the incident light in SiO_2 and 2 is the refracted light in silicon. The angle of incidence $i=90-\theta$, and the refraction angle could be expressed:

$$r = \arcsin\left(\frac{n_{SiO_2}}{n_{Si}} \sin i\right) \tag{3}$$

where n_{SiO2} and n_{Si} are the refractive index of SiO_2 and silicon. According to Fresnel formulas [21], the relationship between refracted light and incident light is written as:

$$\frac{E_2}{E_1} = \begin{cases} \dfrac{2\sin(r)\cos(i)}{\sin(i+r)}, & \text{for } s\text{–polarization} \\ \dfrac{2\sin(r)\cos(i)}{\sin(i+r)\cos(i-r)}, & \text{for } p\text{–polarization} \end{cases} \tag{4}$$

where E_1 and E_2 represent the electric fields of incident light and refracted light, and s and p are the two polarizations of light, respectively. The ratios between refracted and incident light, including $|E_2/E_1|^2$ for s (black, square) and p (black, circle) polarizations, versus the angle θ are shown in Fig. 8(c). The two red lines in Fig. 8(c) represent the losses introduced by refraction ($\beta_r = 10^*\log(1-|E_2/E_1|^2)$) for s (square) and p (circle), respectively. Because the incident light is quasi-TE polarization, the case in experiment is close to p in Fig. 8. More precisely, the loss β_r in experiment is between that of s and p. The results show that as θ increases, the refractive light power would increase. According to the experimental results, if $\theta = 12°$, $|E_2/E_1|^2 = 0.03$ for s and 0.09 for p, and the loss due to refraction (β_r) is 0.13–0.40 dB. From the calculations, it is clear that the loss due to refraction would increase with the oblique angle. And the loss of coupling structure would be higher. So, the angle θ is also limited in order to achieve low coupling loss.

According to the experimental results and the analysis, the low coupling loss could be achieved when the coupling structure is in a certain region (Fig. 7). And if the objective mode size is "narrow" (<5 μm), the low loss (<1 dB) coupling could be achieved through the proper design. The coupling would be harder as the size of the mode increases (w increases), which is actually obvious.

4. Conclusions

In this paper, we have demonstrated a low loss coupling structure of silicon slot waveguide operating at the wavelength of 1064 nm. As a preliminary work, a set of transfer waveguides with widths of 2 μm~6 μm are adopted to take the place of silicon emitters. The coupling losses between slot waveguide and transfer waveguides are measured and the loss mechanism of coupling is also analyzed. It is found that there is a "<1 dB" region within combinations of the coupling structural parameters (the length L_c and oblique angle θ). In our special case, the mode width (w) of input light should satisfy $w \approx 2\theta L_c < 5$ μm so that the coupling loss could be less than 1 dB. In other words, for silicon emitters with different mode sizes, the coupling structure should be carefully designed so that lightwave could be coupled into the slot waveguide as much as possible.

Acknowledgments

This work was supported by the National Basic Research Program of China (No. 2011CBA00608), the National Natural Science Foundation of China (Grant nos. 61307068 and 61321004). The authors would like to thank Dr. Wei Zhang, Dr. Dengke Zhang and Dr. Feng Zhu for the valuable discussions and helpful comments.

References

[1] B. Jalali, S. Fathpour, Silicon photonics, IEEE J. Lightwave Technol. 24 (12) (2006) 4600–4615.
[2] N. Daldosso, L. Pavesi, Nanosilicon photonics, Laser Photonics Rev. 3 (6) (2009) 508–534.
[3] Richard Soref, The past, present, and future of silicon photonics, IEEE J. Sel. Top. Quantum Electron. 12 (6) (2006) 1678–1687.
[4] G.M. Lerman, Uriel Levy, Generation of a radially polarized light beam using space-variant subwavelength gratings at 1064 nm, Opt. Lett. 33 (23) (2008) 2782–2784.
[5] X. Li, X. Feng, K. Cui, F. Liu, Y. Huang, Designing low transmission loss silicon

slot waveguide at wavelength band of high material absorption, Opt. Commun. 306 (2013) 131–134.
[6] M.A. Green, J. Zhao, A. Wang, P.J. Reece, M. Gal, Efficient silicon light-emitting diodes, Nature 412 (6849) (2001) 805–808.
[7] K. Cheng, R. Anthony, U.R. Kortshagen, R.J. Holmes, High-efficiency silicon nanocrystal light-emitting devices, Nano Lett. 11 (5) (2011) 1952–1956.
[8] S. Saito, D. Hisamoto, H. Shimizu, H. Hamamura, R. Tsuchiya, Y. Matsui, T. Mine, T. Arai, N. Sugii, K. Torii, S. Kimura, T. Onai, Silicon light-emitting transistor for on-chip optical interconnection, Appl. Phys. Lett. 89 (16) (2006).
[9] C. Xiong, A. Witkowska, S.G. Leon-Saval, T.A. Birks, W.J. Wadsworth, Enhanced visible continuum generation from a microchip 1064nm laser, Opt. Express 14 (13) (2006) 6188–6193.
[10] Y. Ozaki, A. Mizuno, H. Sato, K. Kawauchi, S. Muraishi, Biomedical application of near-infrared Fourier transform Raman spectroscopy, Appl. Spectrosc. 46 (3) (1992) 533–536.
[11] K.C. Neuman, S.M. Block, Optical trapping, Rev. Sci. Instrum. 75 (9) (2004) 2787–2809.
[12] E.D. Palik., Handbook of Optical Constants of Solids, Harcourt Brace Jovanovich, San Diego, 1985.
[13] X. Li, X. Feng, X. Xiao, K. Cui, F. Liu, Y. Huang, Experimental demonstration of silicon slot waveguide with low transmission loss at 106 nm, Opt. Commun. 329 (2014) 168–172.
[14] C. Koos1, P. Vorreau1, T. Vallaitis1, P. Dumon, W. Bogaerts, R. Baets, B. Esembeson, I. Biaggio, T. Michinobu, F. Diederich, W. Freude, J. Leuthold, All-optical high-speed signal processing with silicon–organic hybrid slot waveguides, Nat. Photonics 3 (4) (2009) 216–219.
[15] A.H.J. Yang, S.D. Moore, B.S. Schmidt, M. Klug, M. Lipson, D. Erickson, Optical manipulation of nanoparticles and biomolecules in sub-wavelength slot waveguides, Nature 457 (7225) (2009) 71–75.
[16] C.F. Carlborg, K.B. Gylfason, A. Kazmierczak, F. Dortu, M.J. Banuls Polo, A. Maquieira Catala, G.M. Kresbach, H. Sohlstrom, T. Moh, L. Vivien, J. Popplewell, G. Ronan, C.A. Barrios, G. Stemmea, W. van der Wijngaarta, A packaged optical slot-waveguide ring resonator sensor array for multiplex label-free assays in labs-on-chips, Lab Chip 10 (3) (2010) 281–290.
[17] Carlos Angulo Barrios, Optical slot-waveguide based biochemical sensors, Sensors 9 (6) (2009) 4751–4765.
[18] V.R. Almeida, Q. Xu, C.A. Barrios, M. Lipson, Guiding and confining light in void nanostructure, Opt. Lett. 29 (11) (2004) 1209–1211.
[19] S. Zhu, T.Y. Liow, G.Q. Lo, D.L. Kwong, Silicon-based horizontal nanoplasmonic slot waveguides for on-chip integration, Opt. Express 19 (9) (2011) 8888–8902.
[20] L. Chen, J. Shakya, M. Lipson, Subwavelength confinement in an integrated metal slot waveguide on silicon, Opt. Lett. 31 (14) (2006) 2133–2135.
[21] E. Hecht., Optics, Addison-Wesley Professional, Boston, 2002.